



Birkbeck ePrints: an open access repository of the research output of Birkbeck College

<http://eprints.bbk.ac.uk>

Thompson, Katherine C. and Margey, Paula (2003) Hydrogen bonded complexes between nitrogen dioxide, nitric acid, nitrous acid and water with SiH_3OH and $\text{Si}(\text{OH})_4$. *Physical Chemistry Chemical Physics* **5** (14) 2970-2975.

This is an author-produced version of a paper published in *Physical Chemistry Chemical Physics* (ISSN 1463-9076). This version has been peer-reviewed but does not include the final publisher proof corrections, published layout or pagination.

All articles available through Birkbeck ePrints are protected by intellectual property law, including copyright law. Any use made of the contents should comply with the relevant law.

Citation for this version:

Thompson, Katherine C. and Margey, Paula (2003) Hydrogen bonded complexes between nitrogen dioxide, nitric acid, nitrous acid and water with SiH_3OH and $\text{Si}(\text{OH})_4$. *London: Birkbeck ePrints*. Available at: <http://eprints.bbk.ac.uk/archive/00000237>

Citation for the publisher's version:

Thompson, Katherine C. and Margey, Paula (2003) Hydrogen bonded complexes between nitrogen dioxide, nitric acid, nitrous acid and water with SiH_3OH and $\text{Si}(\text{OH})_4$. *Physical Chemistry Chemical Physics* **5** (14) 2970-2975.

<http://eprints.bbk.ac.uk>

Contact Birkbeck ePrints at lib-eprints@bbk.ac.uk

Hydrogen bonded complexes between nitrogen dioxide, nitric acid, nitrous acid and water with SiH₃OH and Si(OH)₄

Katherine C. Thompson* and Paula Margey

Division of Physical and Inorganic Chemistry, Carnelley Building, University of Dundee, Dundee DD1 4HN, UK.

** Present address School of Biological and Chemical Sciences, Birkbeck University of London, Gordon House, 29 Gordon Square, London, WC1H 0PP*

Abstract

The inter-conversion of nitrogen oxides and oxy acids on silica surfaces is of major atmospheric importance. As a preliminary step towards rationalising experimental observations, and understanding the mechanisms behind such reactions we have looked at the binding energies of NO₂, N₂O₄, HNO₃, HONO and H₂O with simple proxies of a silica surface, namely SiH₃OH and Si(OH)₄ units. The geometries of these molecular clusters were optimised at both HF/6-311+G(d) and B3LYP/6-311+G(d) level of theory. The SCF energies of the species were determined at the HF/6-311++G(3df,2pd) and B3LYP/6-311++G(3df,2pd) level. The values indicate that nitric acid is by far the most strongly bound species, in agreement with experimental observations. It was also found that the dimer N₂O₄ is significantly more strongly bound to the Si(OH)₄ and SiH₃OH units than NO₂ itself. The vibrational frequencies calculated for the hydrogen-bonded complexes are compared to the experimentally observed frequencies of the adsorbed species were possible.

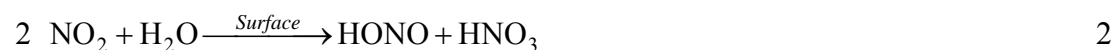
Introduction

The hydroxyl radical, OH, drives the daytime gas phase oxidation of organic compounds in the atmosphere.¹ Accurate values for the rates of formation and loss of OH radicals are therefore central to the development of reliable air quality models. The photolysis of gas phase nitrous acid, HONO:



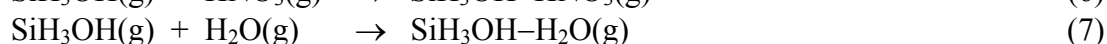
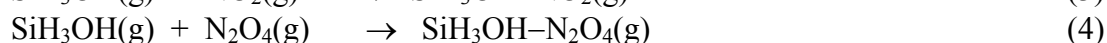
is a major source of OH radicals in the early morning hours, with production rates of up to 5×10^7 molecule $\text{cm}^{-3} \text{s}^{-1}$ of OH radicals calculated from measured HONO concentrations.² The concentration of HONO in the troposphere is, however, difficult to estimate as the reactions that form HONO are themselves poorly understood,³ thus making it difficult to predict OH concentrations. Twenty years ago it was observed that NO_2 reacts in the presence of water vapour and an interface to form HONO.⁴ Since then a number of groups have studied the reaction in the presence of a silica surface (SiO_2), these studies are summarised in the papers by Grassian⁵ and Finlayson-Pitts *et al.*⁶ As silicates are a major component of wind blown mineral dusts and building materials,⁶ there is an ample source of SiO_2 surfaces in the atmosphere.

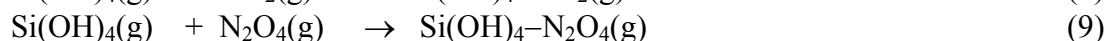
The stoichiometry of the heterogeneous reaction between NO_2 and H_2O is believed to be:



and the reaction is reported to be first order with respect to both NO_2 and H_2O .⁷ Several experimental studies have confirmed that the reaction does indeed lead to the production of gas phase HONO. Gas phase HNO_3 has not been observed as a reaction product, but recent spectroscopic studies have observed HNO_3 adsorbed onto the silica surface,^{8,9} and older studies reported the presence of NO_3^- ions in surface washings.^{10,11} Proposed mechanisms for the formation of HONO on silica surfaces involve N_2O_4 , rather than NO_2 , as the adsorbed species that reacts to yield gas phase HONO.⁶

Surface catalysed reactions often involve the initial formation of a hydrogen bonded adduct with the surface. On a silica surface this will usually involve an interaction between the surface hydroxyl groups and the reactant species. Silanol, SiH_3OH , and orthosilicic acid, $\text{Si}(\text{OH})_4$, provide much simplified models to study the interactions of these hydroxyls groups with the reactant species.¹² In order to understand the mechanism of reaction (2) we have used computational methods to determine values for $\Delta_r H_{298 \text{ K}}$ for the following systems at 1 atmosphere pressure:





The vibrational frequencies, and especially the shifts in the vibrational frequencies of the species in the hydrogen-bonded complexes relative to the free species, were also predicted. A number of studies have shown that the minimal model for the silica surface, SiH_3OH , gives accurate predictions of the shifts in vibrational frequencies observed experimentally when species bond to real silica surfaces, if the computational method used is of sufficient quality: the method chosen must include the effects of electron correlation (post-SCF or DFT methods) and a relatively large basis set must be employed.¹³

Computational Details

All calculations were performed using the Gaussian-98 suite of programs¹⁴ running on a Sun Ultra-80 machine. Geometry optimizations were carried out at both HF and B3LYP^{15,16} level using the basis set 6-311+G(d). A frequency calculation was performed for all stationary points located, using the same method and basis set. Single point energies were carried out on all structures that corresponded to minima on the potential energy surface for the systems using the basis set 6-311++G(3df,2pd), with the convergence for the SCF calculations specified as Tight.

The values of $\Delta_r H$ calculated in this work will be slightly larger than the true values due to the Basis Set Superposition Error, BSSE. In a complex AB the calculated energy of species A, in the complex geometry, will be lower than the energy calculated for A, in the complex geometry in the absence of B, because in the complex A can compensate for deficiencies in its own basis set by making use of functions centred on B, the same is of course true for species B. The counterpoise correction, CP, described in most standard texts (for instance Jensen¹⁷) provides an estimate, or rather an upper limit, on the error caused by the BSSE.

Results and Discussion

The optimised geometries of the lowest energy structures located at the B3LYP/6-311+G(d) level of theory for complexes between Si(OH)_4 and HNO_3 , HONO, NO_2 , N_2O_4 and H_2O are shown in figure 1. Figure 2 shows the lowest energy structures located for complexes between SiH_3OH and HNO_3 , HONO, NO_2 , N_2O_4 and H_2O for a particular interaction, for example the lowest energy structure for the hydrogen of HNO_3 hydrogen-bonding to the O of SiH_3OH , Type A, and the lowest energy structure for an oxygen of HNO_3 hydrogen-bonding to the alcoholic H of SiH_3OH , Type B, are both shown (it should be noted that a minimum energy structure where the alcoholic hydrogen of SiH_3OH is hydrogen bonded to an O of HONO was not found.) Table 1 shows the absolute energies (SCF) and the energies at 298 K, (obtained using the thermal corrections from the frequency calculations without the use of a scaling factor) for all species shown in figures 1 and 2, and Si(OH)_4 , SiH_3OH , HNO_3 , HONO, NO_2 , N_2O_4 and H_2O themselves. Table 2 gives the values of $\Delta_r H_{298\text{ K}}$ obtained using the values given in Table 1 and including the ΔnRT term to convert from energy to enthalpy differences. The CP corrected enthalpies obtained at the HF/6-311++G(3df,2pd)//HF/6-311+G(d) level are shown in parentheses in Table 2.

The most striking feature of table 2 is that the dimer N_2O_4 is significantly more strongly bound to both $\text{Si}(\text{OH})_4$ and SiH_3OH units than NO_2 itself. It can also be seen from table 2 that HNO_3 binds more strongly to both $\text{Si}(\text{OH})_4$ and SiH_3OH than either HONO , N_2O_4 or NO_2 , supporting the idea that it may be left bound to the surface if formed during the reaction of NO_2 with water on a silica surface. It should be noted that in this study the only interaction considered has been one that involves the surface OH group of silica, a real silica surface will have other types of potential binding sites and will also allow larger molecules to bond simultaneously to OH groups attached to different Si atoms.

The value of $\Delta_r H_{298\text{ K}}$ obtained when the H of HNO_3 hydrogen-bonds to the oxygen of SiH_3OH (Type A), -32.3 kJ mol^{-1} and to an $\text{Si}(\text{OH})_4$ unit, -35.5 kJ mol^{-1} , may be compared to the value calculated by Kjaergaard¹⁸ for HNO_3 binding to an H_2O unit, -40.4 kJ mol^{-1} (obtained at the B3LYP/6-311++G(2d,2p)//B3LYP/6-311++G(2d,2p)). The value obtained by Kjaergaard for the binding energy of a simple $\text{HNO}_3\text{--H}_2\text{O}$ cluster compares very well to the measured adsorption enthalpy for HNO_3 on crystalline ice, -44 kJ mol^{-1} .¹⁹

The value calculated for the binding energy (the difference in the absolute energies shown in Table 1) for the O of H_2O hydrogen-bonding to the alcoholic H of SiH_3OH (Type B), -24.4 kJ mol^{-1} , compares well to the value reported by Civalleris et al.¹³ for this property, -23.1 kJ mol^{-1} , computed at the B3LYP/aug-cc-pVDZ level//B3LYP/aug-cc-pVDZ level. Both the value calculated for $\Delta_r H_{298\text{ K}}$ for this interaction, -23.2 kJ mol^{-1} , and for H_2O hydrogen bonding to $\text{Si}(\text{OH})_4$, -21.4 kJ mol^{-1} , may be compared to the value obtained by Kjaergaard¹⁸ for binding energy of the H_2O dimer, 19.3 kJ mol^{-1} (again calculated at the B3LYP/6-311++G(2d,2p)//B3LYP/6-311++G(2d,2p) level) and the experimentally determined value for $\Delta_r H_{298\text{ K}}$ for the formation of the $(\text{H}_2\text{O})_2$ dimer, $-22.6 \pm 2.9\text{ kJ mol}^{-1}$.²⁰ The binding energies calculated in this work for the $\text{Si}(\text{OH})_4\text{--H}_2\text{O}$ and $\text{SiH}_3\text{OH--H}_2\text{O}$ complexes are significantly lower than the experimentally determined value of the enthalpy change when a monolayer of H_2O adsorbs on an SiO_2 surface, -50.3 kJ mol^{-1} , which is in itself larger than the enthalpy change for the condensation of water vapour -44.0 kJ mol^{-1} .²¹

The Table 3 gives the harmonic vibrational frequencies calculated for the complexes involving nitric acid, nitric acid alone and the experimentally determined fundamental vibrational frequencies of nitric acid in the gas phase. Table 4 gives the equivalent data for N_2O_4 .

Some of the frequencies shown in Table 3 can be compared to those observed when HNO_3 is thought to be hydrogen-bonded to a real silica surface (not all vibrational modes can be observed experimentally owing to experimental limitations). Grassian and co-workers and Finlayson-Pitts and co-workers have looked at the FTIR spectrum of the surface bound species formed when a SiO_2 surface with varying amounts of adsorbed water is exposed to gas phase NO_2 . The two groups reported that an absorption centred at $\sim 1680\text{ cm}^{-1}$, (1677 cm^{-1} ,⁸ and 1680 cm^{-1} ,⁹) was observed. The band was attributed to molecularly adsorbed nitric acid (assigned by Grassian to the asymmetric stretch of the NO_2 unit in surface bound HNO_3 .) The Grassian group

also reported that spectral features were observed at 1399 cm^{-1} , (assigned by Grassian to an in-plane OH bend, described as “Mixed” in table 3 and corresponds to the experimentally observed peak for gas phase HNO_3 at 1325.74 cm^{-1}) and 1315 cm^{-1} (assigned by Grassian to an NO_2 stretch, again described as “Mixed” in table 3 and corresponds to the experimentally observed peak for gas phase HNO_3 at 1303.52 cm^{-1} .)

The band observed by the two experimental studies at $\sim 1680\text{ cm}^{-1}$ is shifted by about -30 cm^{-1} from the position observed experimentally for gas phase HNO_3 . The calculations performed in this work show that when HNO_3 is hydrogen bonded to a $\text{Si}(\text{OH})_4$ unit the position of the NO_2 asymmetric stretch is shifted by -25 cm^{-1} , in good agreement with the experimental data. The weaker complexes formed between HNO_3 and SiH_3OH units show a smaller predicted shift for this vibrational frequency, -13 (Type A) and -10 cm^{-1} (Type B), perhaps indicating that HNO_3 forms a stronger hydrogen-bond or combination of hydrogen-bonds with the surface of SiO_2 than that predicted using the simple proxy SiH_3OH , where only one hydrogen-bond may be formed.

The band observed by Grassian at 1399 cm^{-1} , assigned to the out of plane bend of the OH unit, is shifted by $+73\text{ cm}^{-1}$ relative to gas phase nitric acid. The results of our calculations on the complex $\text{Si}(\text{OH})_4\text{-HNO}_3$ show that this vibrational frequency is expected to shift $+112\text{ cm}^{-1}$, again in reasonable agreement with the experimental result of Grassian. The calculated shifts for the weaker complexes formed between HNO_3 and SiH_3OH show poorer agreement, the predicted shift in the vibrational frequency of the out of plane bend of the OH group for the $\text{SiH}_3\text{OH-HNO}_3$ (Type A) complex is overestimated at $+134\text{ cm}^{-1}$, and for the Type B complex is underestimated at $+32\text{ cm}^{-1}$.

The peak assigned as the NO_2 stretching vibration of HNO_3 by Grassian, recorded for surface bound HNO_3 as 1315 cm^{-1} (shifted by $+11\text{ cm}^{-1}$ from a gas phase position of 1303.52 cm^{-1}), is correctly predicted by the cluster calculations performed in this study to be only slightly shifted from the gas phase positions: for the $\text{Si}(\text{OH})_4\text{-HNO}_3$ cluster a shift of $+2\text{ cm}^{-1}$ is calculated, for the $\text{SiH}_3(\text{OH})\text{-HNO}_3$ clusters by $+5$ (Type A) and $+1\text{ cm}^{-1}$ (Type B) is calculated.

Neither the Grassian nor the Finlayson-Pitts groups report bands attributed to surface adsorbed NO_2 , however, this may be because the bands are masked by absorbances due to the silica support (which absorbs strongly between ~ 1610 and 1660 cm^{-1} , the region where gas phase NO_2 absorbs most strongly).⁹ The very weakly bound complex between NO_2 and $\text{Si}(\text{OH})_4$ located in this work indicates that surface adsorbed NO_2 would have vibrational frequencies shifted only very slightly (less than 10 cm^{-1}) to higher wavenumbers than that of gas phase NO_2 . Both experimental groups observe bands that they attribute to surface bound N_2O_4 . The Finlayson-Pitts group attribute a band centred at 1740 cm^{-1} to $\text{N}_2\text{O}_{4(\text{ads})}$ and the Grassian group report bands at 1744 cm^{-1} and 1265 cm^{-1} . The band at $\sim 1740\text{ cm}^{-1}$ is shifted by about -17 cm^{-1} with respect to gas phase N_2O_4 , assuming it corresponds purely to the gas phase peak observed at 1757 cm^{-1} . Interestingly, the calculations show that the frequency for this vibration of N_2O_4 is shifted by $+7\text{ cm}^{-1}$ in the $\text{Si}(\text{OH})_4\text{-N}_2\text{O}_4$ cluster, and is shifted by $+2\text{ cm}^{-1}$ in the $\text{SiH}_3\text{OH-N}_2\text{O}_4$ cluster, this could suggest that the geometry

of the cluster determined in this work is not representative of the manner in which N_2O_4 binds to a real SiO_2 surface, or that the species absorbing at $\sim 1740\text{ cm}^{-1}$ in the experimental system is not the adsorbed, symmetric dimer N_2O_4 . However, it is perhaps more likely that the band experimentally observed is a combined band of the in-phase asymmetric stretch of N_2O_4 (1757 cm^{-1} in the gas phase) and a contribution from the out-of-phase asymmetric stretch, 1724 cm^{-1} in the gas phase. The out-of-phase asymmetric stretch is not observed in the gas phase but is predicted to have about 10 % of the IR intensity of the in-phase stretch in the $\text{Si}(\text{OH})_4\text{---N}_2\text{O}_4$ complex. The band reported by Grassian at 1265 cm^{-1} is shifted just $+4\text{ cm}^{-1}$ from the position of the in-phase symmetric stretch band for gas phase of N_2O_4 , suggesting that the asymmetric stretching bands should also be very slightly blue shifted. The calculations on the $\text{Si}(\text{OH})_4\text{---N}_2\text{O}_4$ and $\text{SiH}_3\text{OH---N}_2\text{O}_4$ clusters predict that the position of the in-phase symmetric stretching band changes by $+6$ and $+7\text{ cm}^{-1}$ respectively relative to the gas phase.

In conclusion, the change in calculated vibrational frequencies for simple complexes of HNO_3 studied in this work, relative to the calculated gas phase frequencies, lie in good agreement with the experimentally observed peaks, thus reinforcing the assignment of the experimentally observed peaks and validating the simple model, $\text{Si}(\text{OH})_4\text{---HNO}_3$, used here as being a fair representation of HNO_3 bound to a SiO_2 surface. In the case of N_2O_4 the situation is not as clear: the calculations suggest that experimentally observed bands should be slightly blue shifted in the adsorbed species relative to the gas phase species, whilst the experimental results show one peak to be slightly red shifted relative to gas phase N_2O_4 , the other slightly blue shifted.

Conclusions

Binding enthalpies for complexes formed between HNO_3 , HONO , NO_2 , N_2O_4 and H_2O with simple proxies of silica surfaces, namely $\text{Si}(\text{OH})_4$ and SiH_3OH units have been determined. The results are in agreement with proposed mechanisms for reaction (2), in which $\text{N}_2\text{O}_{4(\text{ads})}$, rather than $\text{NO}_{2(\text{ads})}$, is the species which reacts with surface bound water to give HONO and HNO_3 . Our results also indicate that HNO_3 can form strong hydrogen-bonds to the surface and therefore will not be released into the gas phase. Calculated shifts in the vibrational frequencies of HNO_3 and N_2O_4 bound to $\text{Si}(\text{OH})_4$ and SiH_3OH units, relative to the gas phase, are compared with experimentally observed peaks which have been assigned to surface adsorbed HNO_3 and N_2O_4 species. In the case of HNO_3 , the calculated shifts in the peaks agree well with experimental observations, the $\text{Si}(\text{OH})_4$ unit providing the best agreement. In the case of N_2O_4 however, the experimental work suggests that the dominant absorption occurs at a slightly lower wavenumber than in the gas phase whilst the calculations predict that it will occur at a slightly higher wavenumber, possible explanations for this are provided.

Acknowledgements

The authors would like to thank Dr. T. J. Dines for many helpful discussions related to this work.

References

- (1) Wayne, R. P. "*Chemistry of Atmospheres*", Oxford University Press, 2000.
- (2) Winer, A. and Biermann, H. *Res. Chem. Intermed.*, 1994, **20**, 423.
- (3) Lammel G. and Cape, J. N. *Chem. Soc. Rev.*, 1996, **25**, 361.
- (4) Sakamaki, F.; Hatakeyama S. and Akimoto, H. *Int. J. Chem. Kinet.*, 1983, **15**, 1013.
- (5) Grassian, V. H. *J. Phys. Chem. A*, 2002, **106**, 860.
- (6) Finlayson-Pitts, B. J., Wingen, L. M., Sumner, A. L., Syomin, D. and Ramazan, K. A. *Phys. Chem. Chem. Phys.*, 2003, **5**, 223, and references therein.
- (7) Finlayson-Pitts, B. J. and Pitts J. N. Jr., "*Chemistry of the Upper and Lower Atmosphere*", Academic Press, 2000.
- (8) Goodman, A. L.; Underwood, G. M. and Grassian, V. H. *J. Phys. Chem A*, 1999, **103**, 7217.
- (9) Barney W. S. and Finlayson-Pitts, B. J. *J. Phys. Chem. A*, 2000, **104**, 171.
- (10) Svensson, R.; Ljungstrom, E. and Lindqvist, O. *Atmos. Environ.*, 1987, **21**, 1529.
- (11) Febo, A. and Perrino, C. *Atmos. Environ.*, 1991, **25A**, 1055.
- (12) Lasaga, A. C. *Rev. Geophys.*, 1992, **30**, 269.
- (13) Civalleri, B.; Garrone, E. and Ugliengo, P. *J. Phys. Chem. B*, 1998, **102**, 2373.
- (14) Frisch, M.J.; Trucks, G. W.; Schlegel, H. B.; Scuseria, G. E.; Robb, M. A.; Cheeseman, J. R.; Zakrzewski, V. G.; Montgomery, J. A. Jr.; Stratmann, R. E.; Burant, J. C.; Dapprich, S.; Millam, J. M.; Daniels, A. D.; Kudin, K. N.; Strain, M. C.; Farkas, O.; Tomasi, J.; Barone, V.; Cossi, M.; Cammi, R.; Mennucci, B.; Pomelli, C.; Adamo, C.; Clifford, S.; Ochterski, J.; Petersson, G. A.; Ayala, P. Y.; Cui, Q.; Morokuma, K.; Malick, D. K.; Rabuck, A. D.; Raghavachari, K.; Foresman, J. B.; Cioslowski, J.; Ortiz, J. V.; Stefanov, B. B.; Liu, G.; Liashenko, A.; Piskorz, P.; Komaromi, I.; Gomperts, R.; Martin, R. L.; Fox, D. J.; Keith, T.; Al-Laham, M. A.; Peng, C. Y.; Nanayakkara, A.; Gonzalez, C.; Challacombe, M.; Gill, P. M. W.; Johnson, B.; Chen, W.; Wong, M. W.; Andres, J. L.; Gonzalez, C.; Head-Gordon, M.; Replogle, E. S. and Pople, J. A in 'Gaussian 98', Pittsburgh, PA, 1998.
- (15) Becke, A. D. *J. Chem. Phys.*, 1993, **98**, 5648.

- (16) Lee, C. T.; Yang, W. T. and Parr, R. G. *Phys. Rev. B*, 1988, **37**, 785.
- (17) Jensen, F. "*Introduction to Computational Chemistry*", John Wiley & Sons, 1999.
- (18) Kjaergaard, H. G. *J. Phys. Chem. A*, 2002, **106**, 2979.
- (19) Bartels-Rausch, T.; Eichler, B.; Zimmermann, P.; Gäggeler H. W. and Ammann, M. *Atmos. Chem. Phys.*, 2002, **2**, 235.
- (20) Curtiss, L. A.; Frurip, D. J. and Blander, M. *J. Chem. Phys.*, 1979, **71**, 2703.
- (21) Goodman, A. L.; Bernard E. T. and Grassian, V. H. *J. Phys. Chem. A*, 2001, **105**, 6443.
- (22) McGraw, G. E.; Bernitt, D. L. and Hisatsune, I. C. *J. Chem. Phys.*, 1965, **42**, 237.
- (23) Melen, F.; Pokorni, F. and Herman, M. *Chem. Phys. Lett.*, 1992, **194**, 181.

Table 1 Absolute energies calculated at the HF/6-311++G(3df,2pd)//HF/6-311+G(d) and B3LYP/6-311++G(3df,2pd)//B3LYP/6-311+G(d) level of theories

	HF level of theory		B3LYP level of theory	
	Energy / E _h	Energy at 298.15 K / E _h	Energy / E _h	Energy at 298.15 K / E _h
Si(OH) ₄	-591.086818	-591.017714	-593.176484	-593.111892
SiH ₃ OH	-366.206218	-366.161437	-367.223546	-367.178765
HNO ₃	-279.563353	-279.529973	-280.999929	-280.970107
HONO	-204.726003	-204.699714	-205.786318	-205.762907
NO ₂	-204.113525	-204.100788	-205.155264	-205.143544
N ₂ O ₄	-408.203049	-408.171083	-410.332090	-410.303523
H ₂ O	-76.059066	-76.033042	-76.464088	-76.440037
Si(OH) ₄ —HNO ₃	-870.664701	-870.558464	-874.192676	-874.094581
Si(OH) ₄ —HONO	-795.821676	-795.722628	-798.973111	-798.881445
Si(OH) ₄ —NO ₂	-795.203571	-795.118522	-798.334647	-798.255140
Si(OH) ₄ —N ₂ O ₄	-999.297138	-999.192634	-1003.514282	-1003.417774
Si(OH) ₄ —H ₂ O	-667.15459	-667.055113	-669.652298	-669.559144
SiH ₃ OH—HNO ₃ (A type)	-645.780799	-645.699076	-648.235724	-648.160248
SiH ₃ OH—HNO ₃ (B type)	-645.773641	-645.692252	-648.228502	-648.153332
SiH ₃ OH—HONO	-570.940866	-570.865913	-573.019658	-572.950296
SiH ₃ OH—NO ₂	-570.321802	-570.261176	-572.380326	-572.323395
SiH ₃ OH—N ₂ O ₄	-774.415418	-774.335210	-777.560002	-777.485989
SiH ₃ OH—H ₂ O (A type)	-442.270071	-442.195406	-443.693761	-443.623759
SiH ₃ OH—H ₂ O (B type)	-442.272983	-442.198197	-443.696933	-443.626707

Table 2 Binding enthalpies calculated at the HF/6-311++G(3df,2pd)//HF/6-311+G(d) and B3LYP/6-311++G(3df,2pd)//B3LYP/6-311+G(d) level of theories (values in parentheses represent CP-corrected values)

	HF level of theory	B3LYP level of theory
	$\Delta_r H_{298\text{ K}} / \text{kJ mol}^{-1}$	$\Delta_r H_{298\text{ K}} / \text{kJ mol}^{-1}$
Si(OH) ₄ —HNO ₃	-30.76 (-28.00)	-35.50
Si(OH) ₄ —HONO	-16.13 (-14.24)	-19.92
Si(OH) ₄ —NO ₂	-2.53 (-1.04)	-1.70
Si(OH) ₄ —N ₂ O ₄	-12.55 (-9.12)	-8.67
Si(OH) ₄ —H ₂ O	-13.91 (-12.40)	-21.4
SiH ₃ OH—HNO ₃ (A type)	-22.60 (-20.54)	-32.34
SiH ₃ OH—HNO ₃ (B type)*	-4.69 (-3.42)	-14.19
SiH ₃ OH—HONO	-14.98 (-13.67)	-25.11
SiH ₃ OH—NO ₂	+0.28 (+1.16)	+1.58
SiH ₃ OH—N ₂ O ₄	-9.54 (-7.17)	-5.29
SiH ₃ OH—H ₂ O (A type)	-4.91 (-3.91)	-15.49
SiH ₃ OH—H ₂ O (B type)	-12.24 (-11.20)	-23.23

Table 3. Vibrational frequencies of HNO₃ alone and with Si(OH)₄ and SiH₃OH units. All values are in units of cm⁻¹.

HNO ₃ alone*	HNO ₃ alone [§]	HNO ₃ --Si(OH) ₄ [§]	HNO ₃ --SiH ₃ OH Type A [§]	HNO ₃ --SiH ₃ OH Type B [§]	Description
458.23	477.1	850.0	852.8	581.8	Torsion
580.30	589.1	635.8	635.8	606.3	NO ₂ rock
646.83	650.2	694.2	685.2	668.0	NO ₂ scissors
763.15	776.9	781.1	780.5	782.0	Out of plane bend
879.11	898.1	957.6	940.3	915.2	ON str
1303.52	1329.9	1332.0	1335.1	1330.8	Mixed
1325.74	1357.7	1470.1	1491.2	1389.9	Mixed
1709.57	1760.5	1735.4	1747.5	1750.2	NO ₂ a-str
3550.0	3699.5	3173.4	3224.9	3548.4	OH str

*Refers to experimentally measured value (fundamental frequency) in gas phase.²²

[§] Values calculated in this work at B3LYP/6-311+G(d) level of theory.

* It should be noted that in the optimised structure for the SiH₃OH—HNO₃ complex (Type B) the H of HNO₃ is interacting an H on the SiH₃OH unit. As an interaction of this nature (proton-hydride) would not be possible on a real silica surface, the binding energy calculated for this complex will be an overestimate of that for HNO₃ hydrogen bonding to a single hydroxyl group on a real silica surface.

Table 4. Vibrational frequencies of N₂O₄ alone and with Si(OH)₄ and SiH₃OH units. All values are in units of cm⁻¹.

N ₂ O ₄ alone*	N ₂ O ₄ alone [§]	N ₂ O ₄ --Si(OH) ₄ [§]	N ₂ O ₄ --SiH ₃ OH [§]	Description
79	83.1	118.0	107.1	Torsion
265	225.4	235.0	235.9	NO ₂ s-rock
281	292.3	300.5	301.6	N–N str
436	436.6	454.8	455.5	NO ₂ s-wag
498	491.8	504.5	503.6	NO ₂ a-rock
677	673.4	688.0	689.8	NO ₂ a-wag
751	762.3	768.4	769.7	NO ₂ a-bend
812	848.6	854.1	853.7	NO ₂ s-bend
1261	1305.8	1312.0	1313.2	NO ₂ s-str (out of phase)
1382	1447.5	1450.8	1451.2	NO ₂ s-str (in phase)
1724	1794.0	1794.3	1796.5	NO ₂ a-str (out of phase)
1757	1827.3	1834.3	1828.4	NO ₂ a-str (in phase)

*Refers to experimentally measured value (fundamental frequency) in gas phase.²³

[§] Values calculated in this work at B3LYP/6-311+G(d) level of theory.

Figure 1. Minimum energy structures, located at B3LYP/6-311+G(d) level, between Si(OH)_4 and HNO_3 , HONO , NO_2 , N_2O_4 and H_2O . All distances are in Å. H and O refer to atoms associated with the Si(OH)_4 unit, ' indicates an atom associated with the other species. Full structural information is provided as supplementary information.

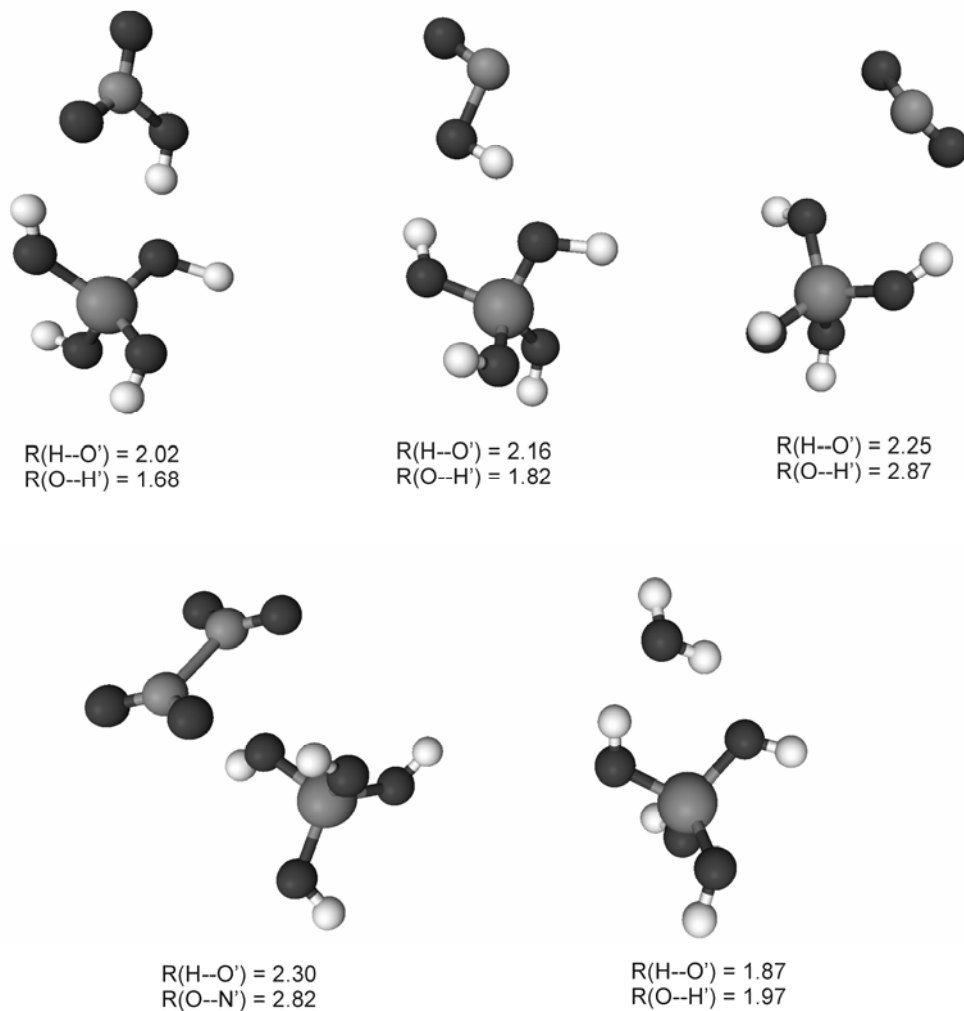


Figure 2. Minimum energy structures located at B3LYP/6-311+G(d) level, between SiH₃OH and HNO₃, HONO, NO₂, N₂O₄ and H₂O. All distances are in Å. H and O refer to atoms associated with the SiH₃OH unit, ' indicates an atom associated with the other species. Full structural information is provided as supplementary information.

